

# A Morphable Face Albedo Model (Supplementary material)

## 1. Lightstage setup

In Figure 1 we show a photo of our lightstage setup. The distribution of cameras is shown in Figure 2 where we also show the three poses captured relative to the camera rig (approximately frontal and two profiles relative to the photometric camera). The camera positioned closest to the equator is our photometric camera for which the polarising filters are tuned. The other seven cameras simply provide additional viewpoints for multiview stereo.

## 2. Demographics

Our model is built from a total of 73 individuals (50 from our own captured data, 23 from the 3DRFE dataset [5]). Of those, 17 are female (6 from 3DRFE). We do not have further demographic information on the 3DRFE participants but show the age distribution for the 50 participants we captured in Figure 3 and skin type in Figure 4.



Figure 1: A subject in our lightstage which comprises white LEDs mounted on a once-subdivided icosahedron.

## 3. Random model samples

To provide another means to compare our model with current state-of-the-art, we draw random faces from each model and render them with a random rotation about the vertical axis drawn uniformly from  $[-30^\circ, 30^\circ]$ . In Figure 5 we show 50 faces from our combined model. In Figure 6 we show 60 faces from the BFM 2017 [2], half with nonlinear gamma applied, half without. The model was not intended to be used with gamma applied but we note that the shading unrealistically severe without. We provide the same visualisation for the LYHM [1] in Figure 7. Our model shows better diversity of skin colour and appearance while leading to model natural rendered appearance comparing to the other models either with or without gamma applied.

## 4. Model visualisation in nonlinear space

A PCA model is a linear subspace model. Diffuse and specular albedo should be statistically modelled in a linear colour space with nonlinear gamma applied subsequently as part of the image formation model. However, we are not used to seeing either linear space face images nor pure albedo images and so the model visualisations look unnatural. To provide another visualisation of our model, in Figure 8 we show our diffuse and specular albedo models with nonlinear gamma applied, i.e. in nonlinear sRGB space.

## 5. Additional qualitative results

We incorporate additional modalities to the figures in the paper to allow a better quantitative comparison of our inverse rendering results in Figure 9 and 10.

## 6. Colour transformation

In Figure 11 we show a plot of  $e$ , the measured light source spectral power distribution for the LEDs used in our lightstage. Note that because our polarising filters are not spectrally neutral, we measure the SPD with the polarisers on the LED. In Figure 12 we show a plot of  $C_r$ ,  $C_g$  and  $C_b$ , the camera spectral sensitivities for the Nikon D200 that we use to capture the photometric images. These were measured by Jiang *et al.* [4]. From these two measurements, we can compute an exact transformation from the RAW colour space captured by our camera to standardised sRGB space.

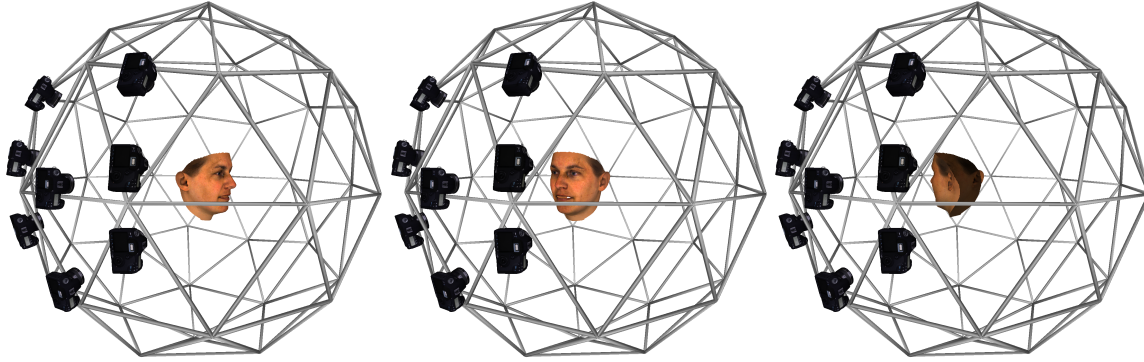


Figure 2: Positioning of cameras in our lightstage. We also show the three poses in which a face is captured, ultimately providing 24 views of the face.

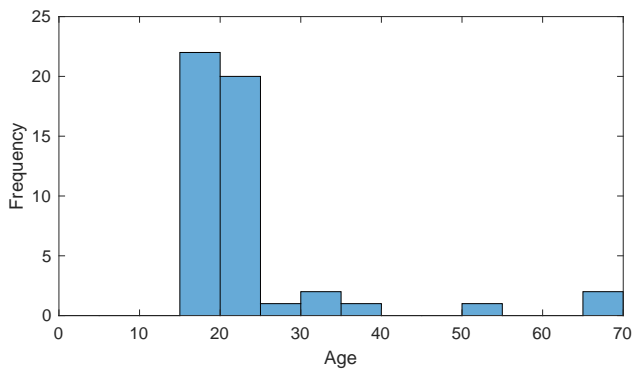


Figure 3: Age distribution for the 50 subjects we captured.

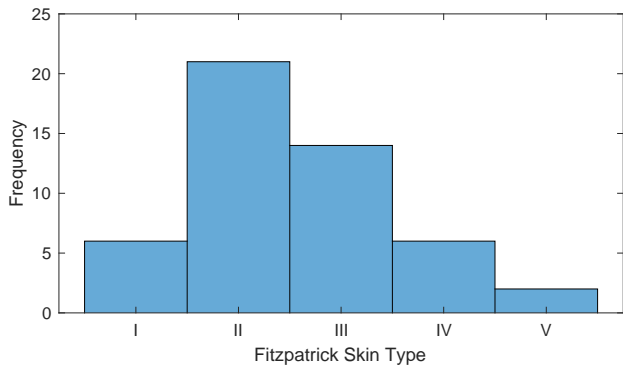


Figure 4: Skin type distribution for the 50 subjects we captured, according to the Fitzpatrick skin type classification.

Since most cameras provide images in this colour space, this means our model can be used to analyse images directly without further colour transformation. For applications in other colour spaces, we provide with our model the measured  $e$  and  $C$  as well as the derived components of the colour transformation matrix that we apply to the albedo maps.

## References

- [1] Hang Dai, Nick Pears, William A. P. Smith, and Christian Duncan. A 3D morphable model of craniofacial shape and texture variation. In *Proc. International Conference on Computer Vision (ICCV)*, 2017. 1, 4
- [2] Thomas Gerig, Andreas Morel-Forster, Clemens Blumer, Bernhard Egger, Marcel Luthi, Sandro Schönborn, and Thomas Vetter. Morphable face models-an open framework. In *Proc. International Conference on Automatic Face and Gesture Recognition*, pages 75–82. IEEE, 2018. 1, 3
- [3] Gary B. Huang, Manu Ramesh, Tamara Berg, and Erik Learned-Miller. Labeled faces in the wild: A database for studying face recognition in unconstrained environments. Technical Report 07-49, University of Massachusetts, Amherst, October 2007. 5
- [4] Jun Jiang, Dengyu Liu, Jinwei Gu, and Sabine Süsstrunk. What is the space of spectral sensitivity functions for digital color cameras? In *Proc. IEEE Winter Conference on Applications of Computer Vision (WACV)*, pages 168–179, 2013. 1
- [5] Giota Stratou, Abhijeet Ghosh, Paul Debevec, and Louis-Philippe Morency. Effect of illumination on automatic expression recognition: a novel 3D relightable facial database. In *Proc. International Conference on Automatic Face and Gesture Recognition*, pages 611–618. IEEE, 2011. 1

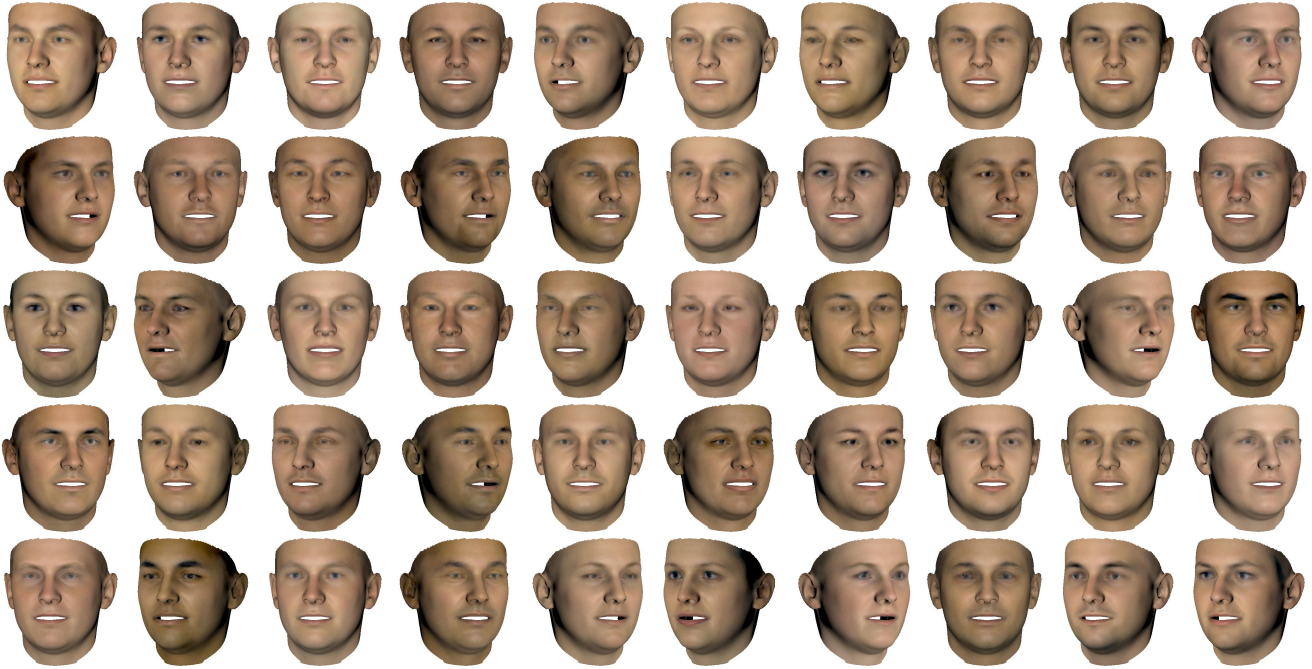


Figure 5: 50 random samples drawn from our combined model and rendered in nonlinear sRGB space with white frontal point light source and Blinn-Phong reflectance with shininess set to 20. In all cases the shape is fixed to the BFM 2017 mean.



Figure 6: 50 random samples drawn from the BFM 2017 [2]. We render with white frontal point light source and Blinn-Phong reflectance with shininess set to 20. In rows 1-3 we apply nonlinear gamma, in 4-6 we do not. We set the specular albedo to the average of the mean specular albedo map in our model. In all cases the shape is fixed to the BFM 2017 mean.

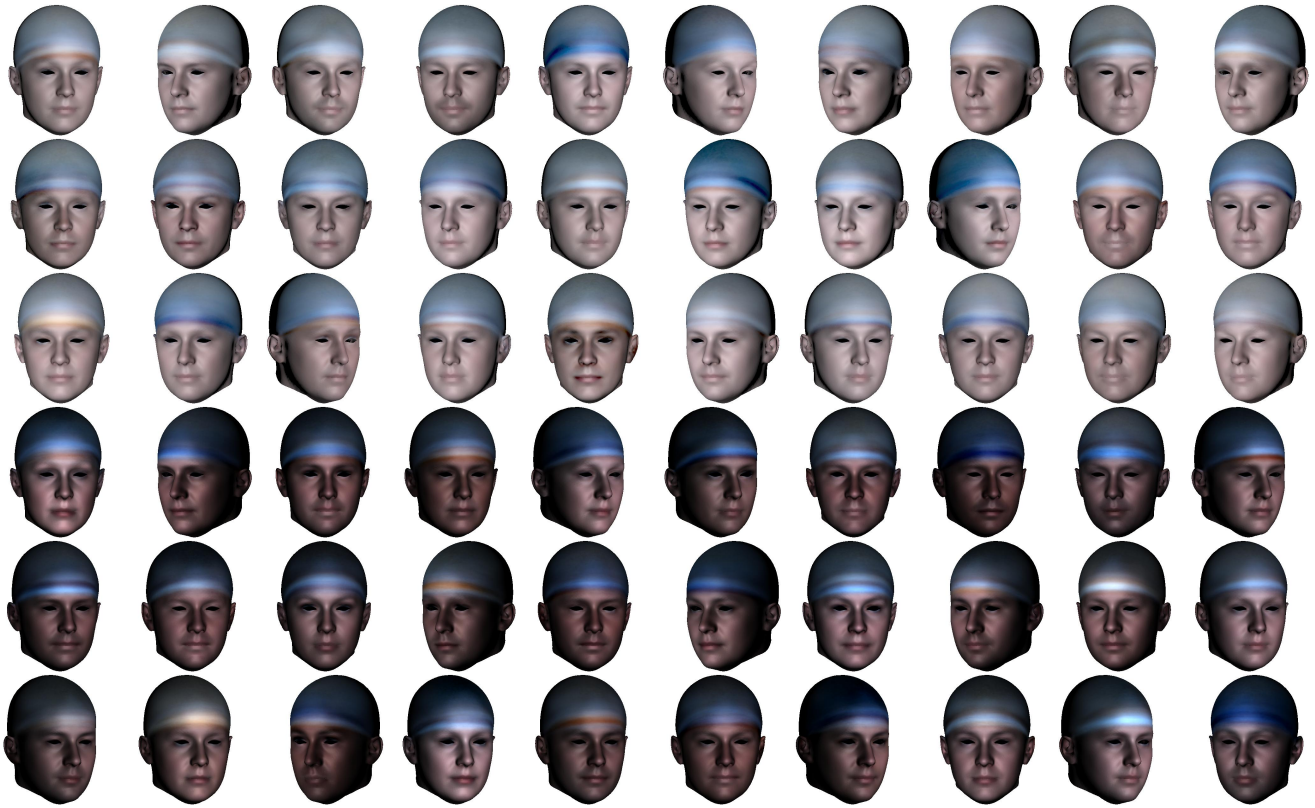


Figure 7: 50 random samples drawn from the LYHM [1]. We render with white frontal point light source and Blinn-Phong reflectance with shininess set to 20. In rows 1-3 we apply nonlinear gamma, in 4-6 we do not. We set the specular albedo to the average of the mean specular albedo map in our model. In all cases the shape is fixed to the LYHM mean.

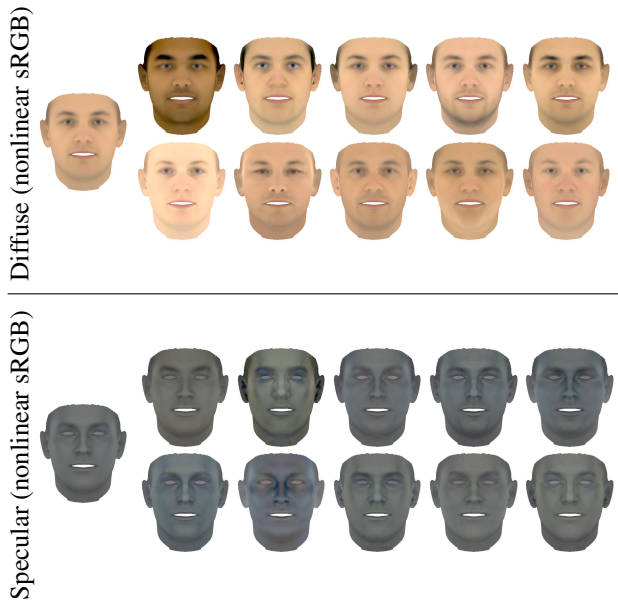


Figure 8: Visualisation of our diffuse and specular albedo models in nonlinear sRGB space.

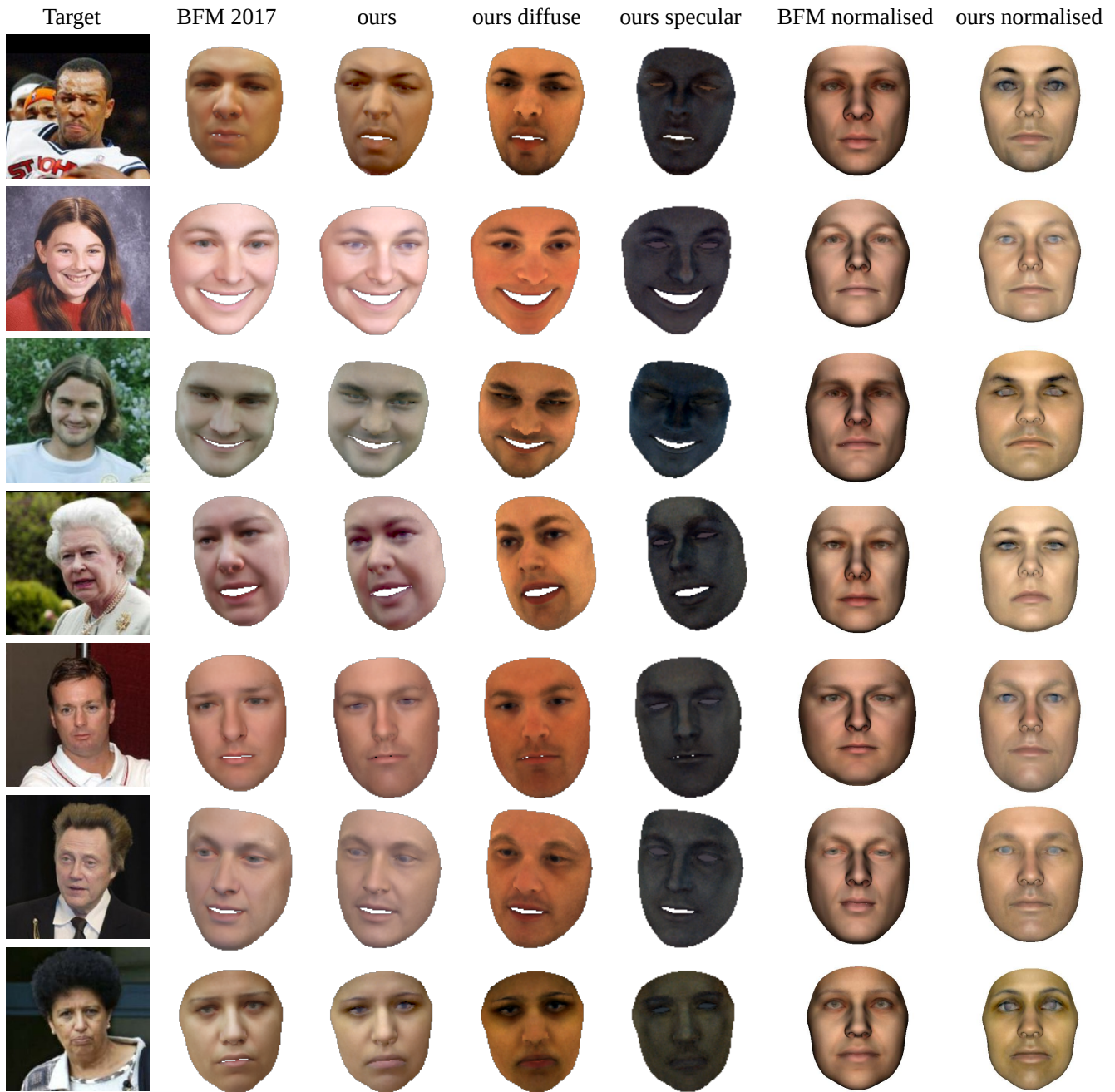


Figure 9: Qualitative model adaptation results on the LFW dataset [3]. Our model leads to comparable results whilst explicitly disentangling albedo and estimating diffuse and specular albedo. We visualize both reconstructions under frontal pose and illumination in the normalised setting.

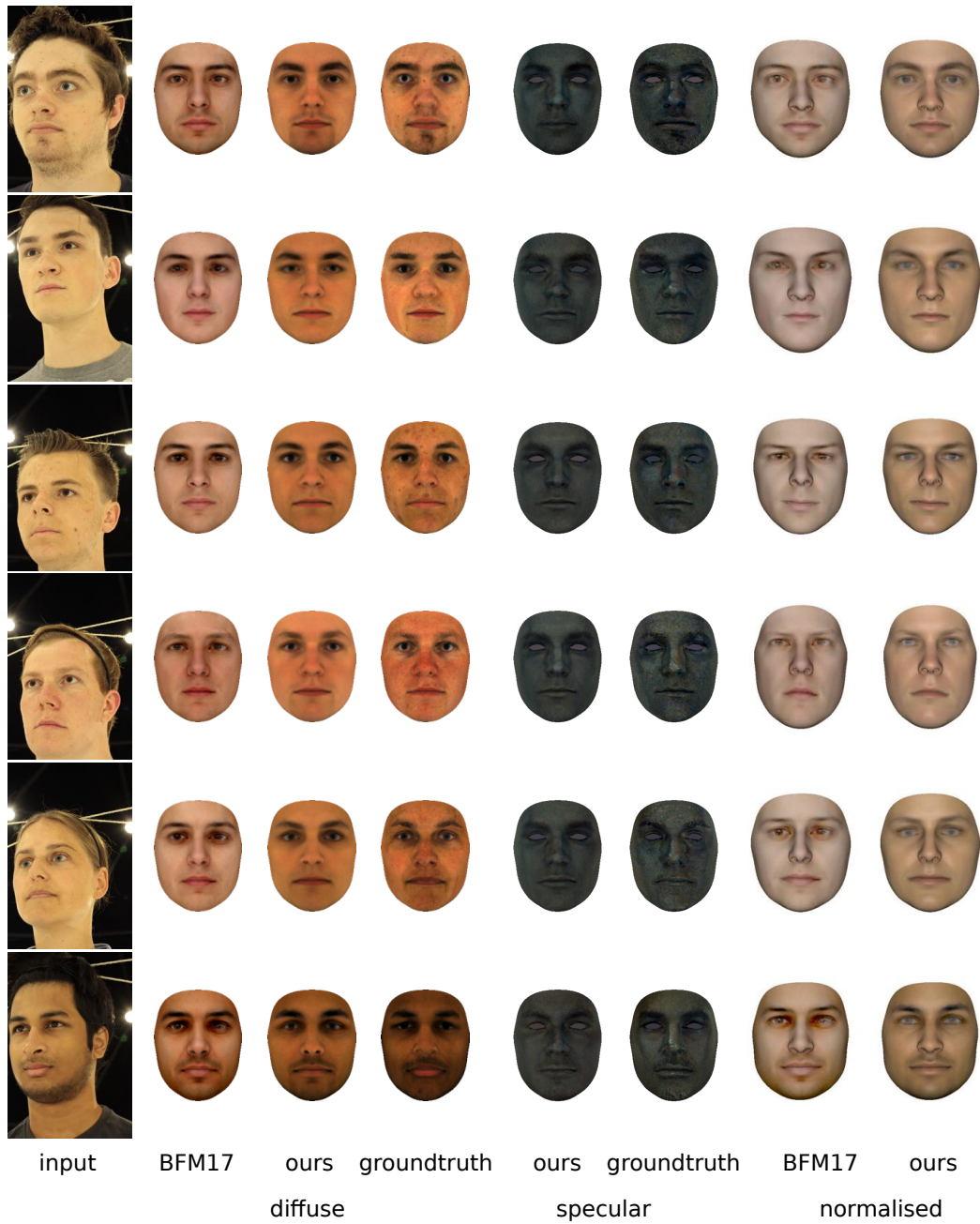


Figure 10: Albedo estimation results based on the exact same inverse rendering pipeline for the BFM 2017 and the proposed model. We present reconstructions of diffuse and specular albedo.

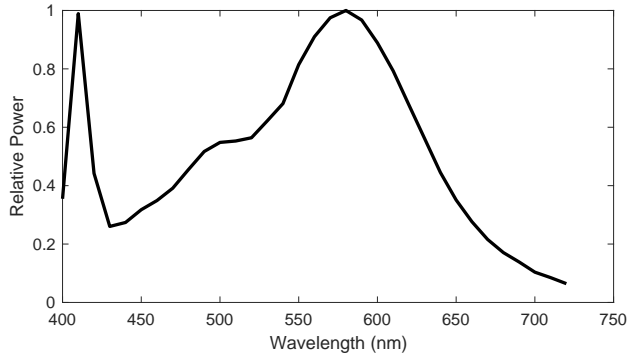


Figure 11: Spectral power distribution of LEDs used in our lightstage.

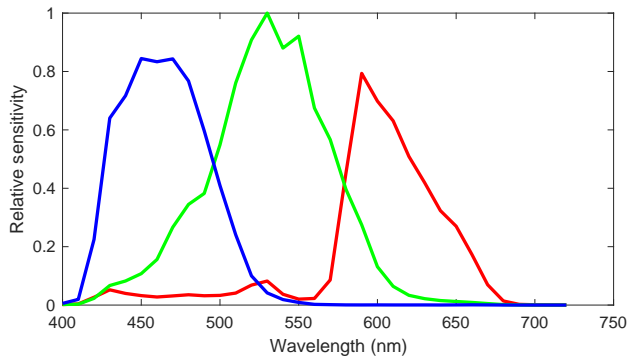


Figure 12: Spectral sensitivity of Nikon D200 used to capture photometric images.